

MICROCOPY RESOLUTION TEST CHART
NATIONAL BUREAU OF STANDARDS-1963-A

AD-A171 085

12

AD



TECHNICAL REPORT BRL-TR-2744

TEMPERATURE AND CONCENTRATION PROFILES
IN HYDROGEN-NITROUS OXIDE FLAMES

John A. Vanderhoff
Steven W. Bunte
Anthony J. Kotlar
Richard A. Beyer

July 1986

DTIC
ELECTE
AUG 18 1986
S D

DTIC FILE COPY

APPROVED FOR PUBLIC RELEASE; DISTRIBUTION UNLIMITED.

US ARMY BALLISTIC RESEARCH LABORATORY
ABERDEEN PROVING GROUND, MARYLAND

86 8 18 062

UNCLASSIFIED

SECURITY CLASSIFICATION OF THIS PAGE (When Data Entered)

REPORT DOCUMENTATION PAGE		READ INSTRUCTIONS BEFORE COMPLETING FORM
1. REPORT NUMBER Technical Report BRL-TR-2744	2. GOVT ACCESSION NO. AD-A171085	3. RECIPIENT'S CATALOG NUMBER
4. TITLE (and Subtitle) TEMPERATURE AND CONCENTRATION PROFILES IN HYDROGEN-NITROUS OXIDE FLAMES		5. TYPE OF REPORT & PERIOD COVERED Final
		6. PERFORMING ORG. REPORT NUMBER
7. AUTHOR(s) John A. Vanderhoff, Steven W. Bunte, Anthony J. Kotlar, Richard A. Beyer		8. CONTRACT OR GRANT NUMBER(s)
9. PERFORMING ORGANIZATION NAME AND ADDRESS US Army Ballistic Research Laboratory ATTN: SLCBR-IB Aberdeen Proving Ground, MD 21005-5066		10. PROGRAM ELEMENT, PROJECT, TASK AREA & WORK UNIT NUMBERS 1L161102AH43
11. CONTROLLING OFFICE NAME AND ADDRESS U.S. Army Ballistic Research Laboratory ATTN: SLCBR-DD-T Aberdeen Proving Ground, MD 21005-5066		12. REPORT DATE July 1986
		13. NUMBER OF PAGES 22
14. MONITORING AGENCY NAME & ADDRESS (if different from Controlling Office)		15. SECURITY CLASS. (of this report) Unclassified
		15a. DECLASSIFICATION DOWNGRADING SCHEDULE NA
16. DISTRIBUTION STATEMENT (of this Report) Approved for Public Release; Distribution Unlimited.		
17. DISTRIBUTION STATEMENT (of the abstract entered in Block 20, if different from Report)		
18. SUPPLEMENTARY NOTES Paper published in <u>Combustion and Flame</u>		
19. KEY WORDS (Continue on reverse side if necessary and identify by block number) H /N O Flames Temperature Profiles Concentration Profiles Raman Spectroscopy		
20. ABSTRACT (Continue on reverse side if necessary and identify by block number) meg Spontaneous Raman spectroscopy has been used to measure temperature and NO, O, and N concentration profiles in lean to stoichiometric premixed laminar hydrogen-nitrous oxide flames. Relative concentration profiles for OH were also obtained for these flames by use of laser induced fluorescence. The present NO concentration results for the stoichiometric flame agree with previous NO measurements obtained by a different optical technique. Profiling these species for various equivalence ratios provides a further		

DD FORM 1 JAN 73 1473 EDITION OF 1 NOV 65 IS OBSOLETE

UNCLASSIFIED

SECURITY CLASSIFICATION OF THIS PAGE (When Data Entered)

UNCLASSIFIED

SECURITY CLASSIFICATION OF THIS PAGE(When Data Entered)

20. Abstract (Cont'd):

test for flame modelers.

UNCLASSIFIED

SECURITY CLASSIFICATION OF THIS PAGE(When Data Entered)

TABLE OF CONTENTS

	<u>Page</u>
I. INTRODUCTION.....	5
II. EXPERIMENTAL.....	5
III. RESULTS.....	6
IV. SUMMARY.....	12
REFERENCES.....	13
DISTRIBUTION LIST.....	15

Accession For	
NTIS CRA&I	<input checked="" type="checkbox"/>
DTIC TAB	<input type="checkbox"/>
Unannounced	<input type="checkbox"/>
Justification	
By	
Distribution /	
Availability Codes	
Dist	Avail and/or Special
A-1	



I. INTRODUCTION

The hydrogen-nitrous oxide flame is of modeling interest as one of the simplest flames which contains nitrogen chemistry; it is also relevant to our area of interest since nitrous oxide is a common propellant oxidizer. Previously, two experimental studies of species and temperature profiles have been reported. Balakhine, et al.,¹ studied a low pressure (0.05 atm.) lean H_2/N_2O flame with a mass spectrometric technique. Cattolica, et al.,² studied an atmospheric pressure stoichiometric flame with laser absorption and fluorescence techniques. We report here, an experimental study of atmospheric pressure H_2/N_2O flames where the equivalence ratio was varied from 0.44 to 1.0. Spontaneous Raman spectroscopy was the primary technique. In addition, laser induced fluorescence was used to obtain relative concentration profiles for OH.

II. EXPERIMENTAL

The apparatus used here has been described in detail previously.³ A nominal 3W Kr^+ laser operating on the 350.742 nm prism selected UV line is used as the excitation source. The laser cavity is extended with curved mirrors providing an intracavity focus where the burner is placed for study. Scattered light from this focused region is imaged on to a 100 μm entrance slit of a 0.25 m monochromator, dispersed and then detected with an intensified Reticon array. The sampled volume of the focal region approximates a cylinder 3 mm long and 100 μm in diameter. To maximize signal the entrance slit is horizontal; that is, its long axis coincides with the laser beam (or long axis of the cylinder). The resolution of the system is about 12 cm^{-1} full width half maximum, which is sufficient to resolve the vibrational structure of the diatomic molecules.

A commercial sintered bronze flat flame burner (McKenna Products) was used for these flame studies. This type of burner is similar to that used by Cattolica, et al.² The 6.0 cm diameter burner head is surrounded by a 7.5 cm diameter shroud through which argon was flowed at a rate of 25 l/min . The reactant gas flow was adjusted to be 15 l/min for all of the equivalence ratios studied. These flows to the burner head are regulated with pressure differences across sintered plugs. The burner is cooled by flowing water through the copper coil imbedded in the sintered plug. Heat extraction is determined from the temperature difference and flow rate of the cooling water.

The N_2 and O_2 calibrations for determining absolute concentration are determined from the ambient room air. For the NO calibration, pure NO gas is flowed through the burner head, as well as argon gas through the shroud. This shroud gas is necessary to minimize formation of NO_2 (which absorbs the laser energy) at the perimeter where the laser beam enters and exits the NO calibration gas. Flames supported by this burner geometry can only be probed to a distance of 0.3 mm from the burner head before the index of refraction gradient deflects the laser beam into the burner head. This deflection also influences the calibration factors for the gases. The collected flame signal has been optimized under these calibration conditions, and since beam position and imaging is slightly different in the flame, a constant factor is applied to all the data of a particular run to correct for the difference. This factor, which typically ranged from 1.2 to 1.3, is determined from a

comparison of the measured N_2 value in the burnt gas region (2-10 mm above the surface) with the calculated value from the NASA-Lewis thermochemical equilibrium code (NLC)⁴ with the code temperature constrained to the measured value. In this comparison, to be discussed later, one-half of the measured NO is included in the N_2 value.

All of the number density profiles have been corrected for the partial masking of the collection optics by the edge of the burner at positions closest to the burner head (0-1.5 mm).

There are several reasons for using the 350.742 nm line of a Kr^+ laser rather than the more standard 514.5 or 488.0 nm lines of an Ar^+ laser for the H_2/N_2O flame studies. First, from previous studies we have found that this line pumps OH and NH and thus relative concentration profiles for these species can be measured using this 350.742 nm line. Second, in the reaction zone vicinity, laser induced fluorescence resulting from either the 514.5 or 488.0 nm pump lines can interfere with the Raman signals.

III. RESULTS

It is possible to observe the Raman spectra simultaneously for four molecules with the experimental detection system. A Raman spectrum indicative of this feature is shown in Figure 1. The Stokes Q-branch rotational-vibrational Raman signals for NO, N_2 , and O_2 are individually analyzed using an interactive multivariate least squares fitting procedure⁵ which incorporates the necessary molecular and experimentally specific information. An analysis of the N_2O Raman signals has not been done. Temperatures obtained from fitting the Raman data for the various molecules are in good agreement, as seen in Table 1. However, since N_2 is present in the largest abundance it is generally used to determine the temperature. Typical temperature fits result in standard deviations of about 1%. Relative concentrations obtained from the fitting are converted to absolute values by comparison to standards. Estimated absolute errors for the temperature measurements are $\pm 3\%$ and $\pm 10\%$ for the concentration measurements of N_2 , O_2 , and NO.

Temperature and concentration results determined from Raman signals produced in an H_2/N_2O flame are contained in Table 1. Here the burner position is fixed such that the laser beam remains 3 mm above the burner surface for all the measurements. For each equivalence ratio there is the adiabatic flame temperature and a comparison of the temperature values obtained from fitting the N_2 , O_2 , and NO signals. As the stoichiometric conditions are approached, the concentrations for O_2 and NO decrease to the point where the fitted temperature has a high degree of uncertainty; however, the temperatures obtained from these different data are generally in good agreement, and much lower than the adiabatic value. Assuming that 3 mm above the burner surface is well into the burnt gas region of the flame a comparison of experimental values with the NLC results can be made. Here, the NLC was constrained to the experimental value of the T_{N_2} for each equivalence ratio in order to account for the substantial heat extraction by the burner.

For most adiabatic flames, the final temperature is the highest at or close to the stoichiometric mixture and falls off with either lean or rich mixtures. The temperature as a function of equivalence ratio (Table 1) does

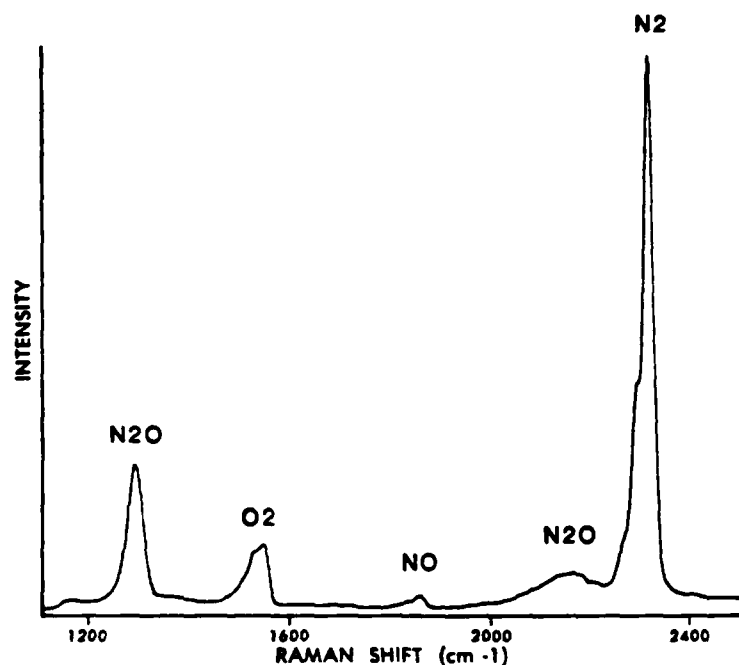


Figure 1. Stokes Q-Branch Raman Spectra of N₂, O₂, NO, and N₂O Occurring in a Hydrogen-Nitrous Oxide Premixed Flame. Laser excitation wavelength is 350.742 nm.

not behave in this manner. Heat extracted from the burner head by the cooling water was measured to vary from 5.0 Kcal/min for the leanest mixture (0.44) to 11.5 Kcal/min for the stoichiometric mixture. An increase in heat extraction indicates the reaction zone of the flame is moving closer to the burner head surface. Thus two opposing effects occur: approaching a stoichiometric mixture increases the flame temperature, but because of the accompanying increase in flame velocity the reaction zone moves closer to the burner surface increasing the heat extraction. The net observed result is that there are similar experimental flame temperatures for all of the equivalence ratios studied.

By assuming all the heat loss is due to conduction to the burner head, a final flame temperature can be calculated.⁶ This has been done for all the equivalence ratios reported here, and the value is constant within the accuracy of the measurement, 2350 ± 100 K. This temperature is $450 \text{ K} \pm 100 \text{ K}$ higher than the experimentally measured values. At $\phi=1.0$, a comparison of heat loss results with those of Cattolica, et al.,² can be made since the burner and experimental conditions are identical. We both determine that about 85% of the heat loss can be accounted for by conduction to the burner head. Cattolica argues that the remaining 15% is due to radiation from the burner surface. At the leanest mixture we find about one-half of the heat loss is due to conduction of the burner head. Now the 450 ± 100 K cannot be due entirely to radiation from the burner surface. Here the burner surface temperature must necessarily be significantly lower since 5.0 rather than 11.5 kcal/min are being extracted. Radiative heat loss from the burnt gases, even

TABLE 1. TEMPERATURE AND SPECIES CONCENTRATIONS IN A H₂/N₂O FLAME FOR VARIOUS EQUIVALENCE RATIOS

ϕ	T _{Ad} (NLC)	T _{N₂}	T _{O₂}	T _{NO}	N ₂	N ₂ (NLC)	O ₂	O ₂ (NLC)	NO	NO(NLC)
	K									
	Mole Per Cent									
0.44	2745	1945	1965	1970	59.6	57.8	14.8	16.0	3.56	0.52
0.45*	2753	1957			59.2	58.0	14.4	16.0	3.46	0.52
0.52	2806	1923	1948	1966	58.3	56.6	12.8	13.4	3.11	0.44
0.60	2855	1898	1919	1959	58.3	55.4	10.7	10.9	2.73	0.37
0.68	2892	1880	1903	1899	55.7	54.2	8.1	8.6	1.99	0.30
0.70*	2900	1886			53.5	54.0	6.6	7.6	1.65	0.29
0.77	2924	1877	1889	1953	50.5	52.9	5.1	5.9	1.93	0.25
0.88	2949	1889	1914	2009	47.9	51.5	2.7	3.1	1.18	0.18
0.89*	2951	1925			50.3	51.2	2.1	2.6	1.38	0.19
1.00	2964	1925	1914		49.2	49.9	0.58	0.09	0.96	0.04

*These values were extracted from the profile measurements shown on Figures 2, 3, and 4 at a burner position of 3 mm.

assuming it is all water vapor, is about an order of magnitude smaller than required. In summary, the heat losses can be accounted for when the gas mixture is close to stoichiometric, but not for the lean mixtures.

The data for N_2 , given in Table 1, show only the excursions of the N_2 concentrations about the NLC values. Experimentally determined concentrations for NO are much larger than those calculated from the NLC and the experimental values for O_2 concentration are generally smaller than those of the NLC. The reason for this is that the experimental flame has not attained complete equilibrium. For a better comparison of the experiment with the NLC values, the NO in excess of the NLC values should be apportioned to the equilibrium products. Concentrations of N_2O at equilibrium are negligible in these flames, thus decreasing NO must increase N_2 . The oxygen from NO can be apportioned to O_2 so the experimental values of O_2 in Table 1 are justifiably low. The exception to this trend is for $\phi=1.0$ where the experimental value for O_2 is much larger than the NLC value. Here, however, the O_2 concentration is so sensitive to the equivalence ratio that uncertainty in the flow of around 2% can by itself produce this difference. Considering the large difference in the experimental and NLC value for the NO concentration, it is obvious that a code containing some detailed chemistry is required to describe this flame system. A direct comparison of experimental results with those of Cattolica, et al.,² can be made at $\phi=1.0$. The flame temperature (1925 K versus 1950 K) and the NO concentration (0.96% versus 1.1%) are in excellent agreement, as expected.

Profile data for H_2/N_2O flames of equivalence ratios 0.45, 0.70, and 0.89 are displayed on Figures 2, 3, and 4, respectively. In addition to the profiles for T, N_2 , O_2 , and NO, the OH relative concentration profile has been obtained from laser induced fluorescence measurements using the same laser excitation line, 350.742 nm. The (0,1) $Q_1(19)$ A-X transition of OH is being pumped and the fluorescence emission of the (0,0) band is monitored. The self absorption effects that occur in this experimental arrangement do not affect the OH relative concentration profiles significantly since the distance over which the self absorption occurs is essentially constant both spatially and with respect to OH density for the various burner positions. With a knowledge of the temperature, the fluorescence intensity can be easily converted to relative concentrations through the Boltzmann factor. The only assumption necessary for the validity of the relative concentration profile is a constant quench rate. This assumption is discussed in detail elsewhere.³

It was thought that a concentration profile for NH might also be obtained for this flame since we have previously been able to excite NH in a CH_4/N_2O flame operating at 2400K.³ However, no NH fluorescence was observed. Cattolica, et al.,² measure a peak NH concentration of 10^{13} molecules/cm³ in an H_2/N_2O stoichiometric flame which is also our estimated sensitivity limit for a 2400K flame.³ The present H_2/N_2O flame temperature is around 500K cooler. Since a high J transition is being pumped, it is not surprising that the NH concentration is below our detection limit. Thus our null result is consistent with the data of Cattolica, et al.²

There are some general features that appear in the profile data of Figures 2, 3, and 4. The temperature profiles are much smoother and scatter free than are the concentration profiles, i.e., the temperature parameter which only depends on the spectral shape is substantially more precise than

the concentration profiles which are signal amplitude sensitive and require a calibration. This is especially true for the region which includes part of the reaction zone (0.3 to 2 mm). Here there can be scatter in the data caused by small laser beam deflections. As the laser beam passes from ambient air into the flame zone, a change in the index of refraction occurs due to the temperature change. If this index of refraction gradient is perpendicular to the propagation of the laser beam, no deflection occurs, however, close to the burner surface the flame edge is curved and deflection does occur. This deflection can move the image on the entrance slit of the monochromator, thus reducing the Raman signal. Should the spatial and spectral resolution requirements be relaxed, i.e., larger entrance slits, the steering effect can be made negligible. Line of sight measurements also have compromised spatial resolution because of this effect. At positions closest to the burner surface the flame temperature is in excess of 1700K showing that the early reaction zone is not being probed under these conditions. The flame temperature peaks around 2 mm and the NO , O_2 , and N_2 concentrations take on constant values from 2 to 10 mm. Thus, these profiles show that the position 3 mm from the burner surface (data of Table 1) is part of the burnt gas region of the flame where, for the most part, equilibrium conditions exist. The exception is that NO remains above its thermochemical equilibrium value. At positions greater than 4 mm from the burner surface, the rate of decrease in OH concentration slows considerably.

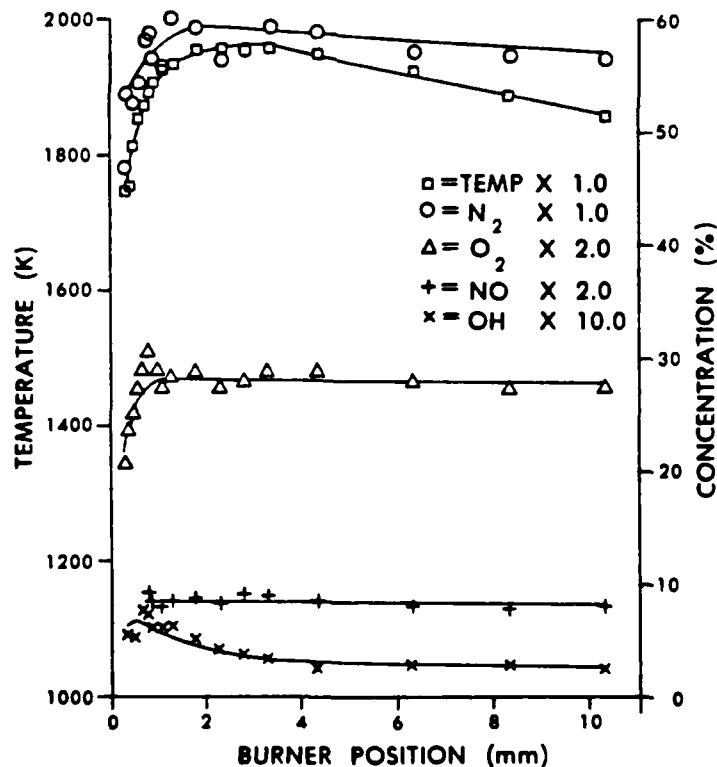


Figure 2. Temperature and Species Concentration Spatial Profiles for N_2 , O_2 , NO , and OH in Hydrogen-Nitrous Oxide Premixed Flames of Equivalence Ratio of 0.45. The solid lines are drawn in to show general trends and clarify the data points.

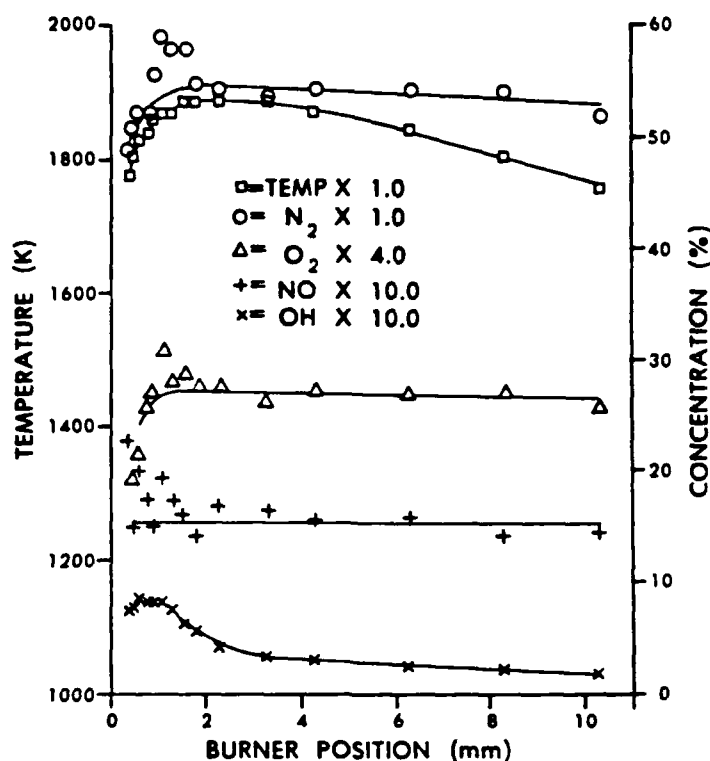


Figure 3. Temperature and Species Concentration Spatial Profiles for N₂, O₂, NO, and OH in Hydrogen-Nitrous Oxide Premixed Flames of Equivalence Ratio of 0.70. The solid lines are drawn in to show general trends and clarify the data points.

Cattolica, et al., find that at positions greater than 6 mm from the burner surface, their measured OH concentrations coincided with the equilibrium values. This information for $\phi=1.0$ lends credence to assuming the OH concentration at a distance of 10 mm from the burner surface is in equilibrium (our results). Now the relative OH concentration profiles can be put on an absolute scale by assigning the 10 mm position the equilibrium value (calculated for the measured temperature at this position), and then normalizing the other points. The equilibrium values are 0.15, 0.08, and 0.06 mole percent for $\phi=0.45$, 0.70, and 0.89, respectively.

Cattolica, et al., measure a peak OH concentration of 0.26 mole percent for an H₂/N₂O stoichiometric flame at T=1950K. We have determined a peak OH concentration of 0.6 mole percent for an H₂/N₂O flame where $\phi=0.89$ and T=1925K. From NLC computations at T=1950K, a change of ϕ from 1.0 to 0.89 increases the OH equilibrium concentration by a factor of 2.3. Use of this correction places our result very close to that of Cattolica, et al. Balakhine, et al., measure a peak OH concentration of 0.06 mole percent for a lean H₂/N₂O flame where $\phi=0.46$, T=1930K and P=0.05 atm. This result is about a factor of 7 below the NLC equilibrium value. The NLC OH equilibrium concentrations for a $\phi=0.45$ and T=1925K H₂/N₂O flame at atmospheric pressure is 0.24 mole percent, and 0.45 mole percent at p=0.05 atm. Our measured relative OH concentrations for the 0.45 and 0.89 equivalence ratios are

similar (within 20% of each other) and the normalized peak concentration is 0.5 mole percent, close to the 0.89 case. Hence, from our method of normalization, there is an order of magnitude difference in the present results and that for the low pressure flame. Although reasons for this difference are not obvious, possible recombination of OH in the sampling nozzle of the low pressure mass spectrometric experiment would result in low OH values.

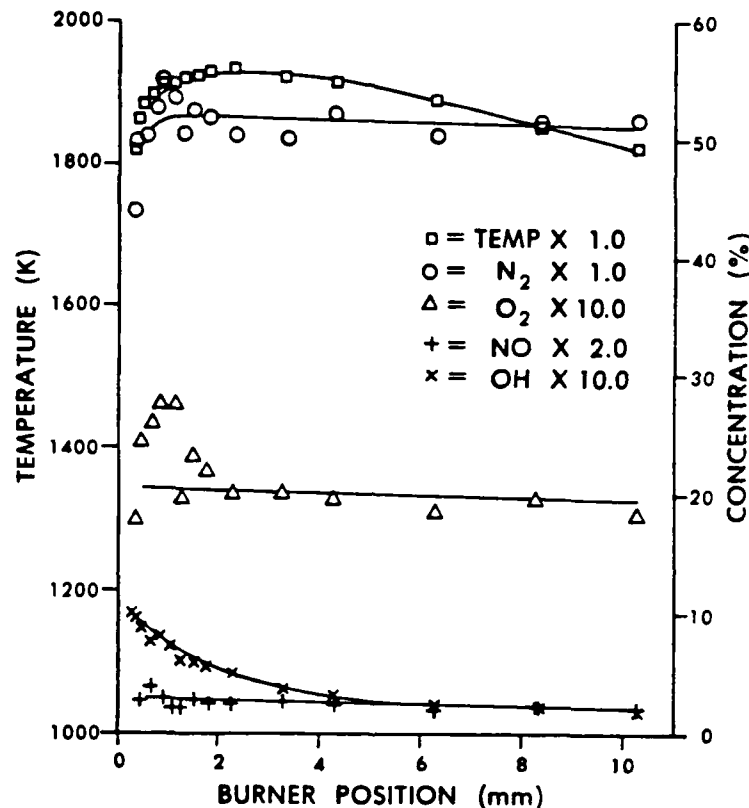


Figure 4. Temperature and Species Concentration Spatial Profiles for N₂, O₂, NO, and OH in Hydrogen-Nitrous Oxide Premixed Flames of Equivalence Ratio of 0.89. The solid lines are drawn in to show general trends and clarify the data points.

IV. SUMMARY

Measured NO concentrations are much higher than the equilibrium values for all the H₂/N₂O flames of the various stoichiometries studied here. These results provide further evidence that detailed chemistry is required to describe this flame system. Both line of sight and spatially resolved optical techniques give similar results for the flame temperature and NO concentration. When comparing the OH concentration of a lean atmospheric pressure H₂/N₂O flame with the same flame operating at low pressure, large differences are observed. Possible pressure effects or the inherent differences of the optical technique with that of mass spectrometric sampling may be responsible.

REFERENCES

1. Balakhine, V.P., Van Dooren, J., and Van Tiggelen, P.J., "Reaction Mechanism and Rate Constants in Lean Hydrogen-Nitrous Oxide Flames," Combustion Flame, Vol. 28, p. 165, 1977.
2. Cattolica, R.J., Smooke, M.D., and Dean, A.M., "A Hydrogen Nitrous Oxide Flame Study," Western States Section of the Combustion Institute, Fall Technical Meeting Paper Number 82-95, 1982.
3. Vanderhoff, J.A., Anderson, W.R., Kotlar, A.J., and Beyer, R.A., "Raman and Fluorescence Spectroscopy in a Methane-Nitrous Oxide Laminar Flame." Proceedings, 20th International Symposium on Combustion, The Combustion Institute, 1984.
4. Svehla, R.A., and McBride, B.J., "Fortran IV Computer Program for Calculation of Thermodynamic and Transport Properties of Complex Chemical Systems," NASA TND-7056, 1973.
5. Wentworth, W.E., "Rigorous Least Squares Adjustment," J. Chem. Ed., Vol. 42, p. 96, 1965.
6. Anderson, W.R., Decker, L.J., and Kotlar, A.J., "Temperature Profile of a Stoichiometric $\text{CH}_4/\text{N}_2\text{O}$ Flame from Laser Excited Fluorescence Measurements on OH," Combustion and Flame, Vol. 48, p. 175, 1982.

DISTRIBUTION LIST

<u>No. Of Copies</u>	<u>Organization</u>	<u>No. Of Copies</u>	<u>Organization</u>
12	Administrator Defense Technical Info Center ATTN: DTIC-DDA Cameron Station Alexandria, VA 22304-6145	1	Commander US Army Aviation Research and Development Command ATTN: AMSAV-E 4300 Goodfellow Blvd. St. Louis, MO 63120
1	HQ DA DAMA-ART-M Washington, DC 20310	1	Director US Army Air Mobility Research and Development Laboratory Ames Research Center Moffett Field, CA 94035
1	Commander US Army Materiel Command ATTN: AMCDRA-ST 5001 Eisenhower Avenue Alexandria, VA 22333-0001	4	Commander US Army Research Office ATTN: R. Ghirardelli D. Mann R. Singleton R. Shaw P.O. Box 12211 Research Triangle Park, NC 27709-2211
10	Central Intelligence Agency Office of Central Reference Dissemination Branch Room GE-47 HQS Washington, DC 20505		
1	Commander Armament R&D Center US Army AMCCOM ATTN: SMCAR-TSS Dover, NJ 07801	1	Commander US Army Communications - Electronics Command ATTN: AMSEL-ED Fort Monmouth, NJ 07703
1	Commander Armament R&D Center US Army AMCCOM ATTN: SMCAR-TDC Dover, NJ 07801	1	Commander ERADCOM Technical Library ATTN: DELSD-L, Reports Section Fort Monmouth, NJ 07703-5301
1	Director Benet Weapons Laboratory Armament R&D Center US Army AMCCOM ATTN: SMCAR-LCB-TL Watervliet, NY 12189	2	Commander Armament R&D Center US Army AMCCOM ATTN: SMCAR-LCA-G, D.S. Downs J.A. Lannon Dover, NJ 07801
1	Commander US Army Armament, Munitions and Chemical Command ATTN: SMCAR-ESP-L Rock Island, IL 61299	1	Commander Armament R&D Center US Army AMCCOM ATTN: SMCAR-LC-G, L. Harris Dover, NJ 07801

DISTRIBUTION LIST

<u>No. Of Copies</u>	<u>Organization</u>	<u>No. Of Copies</u>	<u>Organization</u>
1	Commander Armament R&D Center US Army AMCCOM ATTN: SMCAR-SCA-T, L. Stiefel Dover, NJ 07801	1	Commander US Army Development and Employment Agency ATTN: MODE-TED-SAB Fort Lewis, WA 98433
1	Commander US Army Missile Command Research, Development and Engineering Center ATTN: AMSMI-RD Redstone Arsenal, AL 35898	1	Office of Naval Research Department of the Navy ATTN: R.S. Miller, Code 432 800 N. Quincy Street Arlington, VA 22217
1	Commander US Army Missile and Space Intelligence Center ATTN: AMSMI-YDL Redstone Arsenal, AL 35898-5000	1	Commander Naval Air Systems Command ATTN: J. Ramnarace, AIR-54111C Washington, DC 20360
2	Commander US Army Missile Command ATTN: AMSMI-RK, D.J. Ifshin W. Wharton Redstone Arsenal, AL 35898	2	Commander Naval Ordnance Station ATTN: C. Irish P.L. Stang, Code 515 Indian Head, MD 20640
1	Commander US Army Missile Command ATTN: AMSMI-RKA, A.R. Maykut Redstone Arsenal, AL 35898-5249	1	Commander Naval Surface Weapons Center ATTN: J.L. East, Jr., G-23 Dahlgren, VA 22448-5000
1	Commander US Army Tank Automotive Command ATTN: AMSTA-TSL Warren, MI 48397-5000	2	Commander Naval Surface Weapons Center ATTN: R. Bernecker, R-13 G.B. Wilmot, R-16 Silver Spring, MD 20902-5000
1	Director US Army TRADOC Systems Analysis Activity ATTN: ATAA-SL White Sands Missile Range, NM 88002	1	Commander Naval Weapons Center ATTN: R.L. Derr, Code 389 China Lake, CA 93555
1	Commandant US Army Infantry School ATTN: ATSH-CD-CSO-OR Fort Benning, GA 31905	2	Commander Naval Weapons Center ATTN: Code 3891, T. Boggs K.J. Graham China Lake, CA 93555

DISTRIBUTION LIST

<u>No. Of Copies</u>	<u>Organization</u>	<u>No. Of Copies</u>	<u>Organization</u>
5	Commander Naval Research Laboratory ATTN: M.C. Lin J. McDonald E. Oran J. Shnur R.J. Doyle, Code 6110 Washington, DC 20375	1	NASA Langley Research Center Langley Station ATTN: G.B. Northam/MS 168 Hampton, VA 23365
1	Commanding Officer Naval Underwater Systems Center Weapons Dept. ATTN: R.S. Lazar/Code 36301 Newport, RI 02840	4	National Bureau of Standards ATTN: J. Hastie M. Jacox T. Kashiwagi H. Semerjian US Department of Commerce Washington, DC 20234
1	Superintendent Naval Postgraduate School Dept. of Aeronautics ATTN: D.W. Netzer Monterey, CA 93940	1	OSD/SDIO/UST ATTN: L.H. Caveny Pentagon Washington, DC 20301-7100
4	AFRPL/DY, Stop 24 ATTN: R. Corley R. Geisler J. Levine D. Weaver Edwards AFB, CA 93523-5000	1	Aerojet Solid Propulsion Co. ATTN: P. Micheli Sacramento, CA 95813
1	AFRPL/MKPB, Stop 24 ATTN: B. Goshgarian Edwards AFB, CA 93523-5000	1	Applied Combustion Technology, Inc. ATTN: A.M. Varney P.O. Box 17885 Orlando, FL 32860
1	AFOSR ATTN: J.M. Tishkoff Bolling Air Force Base Washington, DC 20332	2	Applied Mechanics Reviews The American Society of Mechanical Engineers ATTN: R.E. White A.B. Wenzel 345 E. 47th Street New York, NY 10017
1	Air Force Armament Laboratory ATTN: AFATL/DLODL Eglin AFB, FL 32542-5000	1	Atlantic Research Corp. ATTN: M.K. King 5390 Cherokee Avenue Alexandria, VA 22314
		1	Atlantic Research Corp. ATTN: R.H.W. Woesche 7511 Wellington Road Gainesville, VA 22065

DISTRIBUTION LIST

<u>No. Of Copies</u>	<u>Organization</u>	<u>No. Of Copies</u>	<u>Organization</u>
1	AVCO Everett Rsch. Lab. Div. ATTN: D. Stickler 2385 Revere Beach Parkway Everett, MA 02149	1	General Electric Ordnance Systems ATTN: J. Mandzy 100 Plastics Avenue Pittsfield, MA 01203
1	Battelle Memorial Institute Tactical Technology Center ATTN: J. Huggins 505 King Avenue Columbus, OH 43201	2	General Motors Rsch Labs Physics Department ATTN: T. Sloan R. Teets Warren, MI 48090
1	Cohen Professional Services ATTN: N.S. Cohen 141 Channing Street Redlands, CA 92373	2	Hercules, Inc. Allegany Ballistics Lab. ATTN: R.R. Miller E.A. Yount P.O. Box 210 Cumberland, MD 21501
1	Exxon Research & Eng. Co. Government Research Lab ATTN: A. Dean P.O. Box 48 Linden, NJ 07036	1	Hercules, Inc. Bacchus Works ATTN: K.P. McCarty P.O. Box 98 Magna, UT 84044
1	Ford Aerospace and Communications Corp. DIVAD Division Div. Hq., Irvine ATTN: D. Williams Main Street & Ford Road Newport Beach, CA 92663	1	Honeywell, Inc. Government and Aerospace Products ATTN: D.E. Broden/ MS MN50-2000 600 2nd Street NE Hopkins, MN 55343
1	General Applied Science Laboratories, Inc. ATTN: J.I. Erdos 425 Merrick Avenue Westbury, NY 11590	1	IBM Corporation ATTN: A.C. Tam Research Division 5600 Cottle Road San Jose, CA 95193
1	General Electric Armament & Electrical Systems ATTN: M.J. Bulman Lakeside Avenue Burlington, VT 05401	1	IIT Research Institute ATTN: R.F. Remaly 10 West 35th Street Chicago, IL 60616
1	General Electric Company 2352 Jade Lane Schenectady, NY 12309		

DISTRIBUTION LIST

<u>No. Of Copies</u>	<u>Organization</u>	<u>No. Of Copies</u>	<u>Organization</u>
2	Director Lawrence Livermore National Laboratory ATTN: C. Westbrook M. Costantino P.O. Box 808 Livermore, CA 94550	1	Rockwell International Corp. Rocketdyne Division ATTN: J.E. Flanagan/HB02 6633 Canoga Avenue Canoga Park, CA 91304
1	Lockheed Missiles & Space Co. ATTN: George Lo 3251 Hanover Street Dept. 52-35/B204/2 Palo Alto, CA 94304	4	Sandia National Laboratories Combustion Sciences Dept. ATTN: R. Cattolica S. Johnston P. Mattern D. Stephenson Livermore, CA 94550
1	Los Alamos National Lab ATTN: B. Nichols T7, MS-B284 P.O. Box 1663 Los Alamos, NM 87545	1	Science Applications, Inc. ATTN: R.B. Edelman 23146 Cumorah Crest Woodland Hills, CA 91364
1	National Science Foundation ATTN: A.B. Harvey Washington, DC 20550	1	Science Applications, Inc. ATTN: H.S. Pergament 1100 State Road, Bldg. N Princeton, NJ 08540
1	Olin Corporation Smokeless Powder Operations ATTN: V. McDonald P.O. Box 222 St. Marks, FL 32355	3	SRI International ATTN: G. Smith D. Crosley D. Golden 333 Ravenswood Avenue Menlo Park, CA 94025
1	Paul Gough Associates, Inc. ATTN: P.S. Gough 1048 South Street Portsmouth, NH 03801	1	Stevens Institute of Tech. Davidson Laboratory ATTN: R. McAlevy, III Hoboken, NJ 07030
2	Princeton Combustion Research Laboratories, Inc. ATTN: M. Summerfield N.A. Messina 475 US Highway One Monmouth Junction, NJ 08852	1	Textron, Inc. Bell Aerospace Co. Division ATTN: T.M. Ferger P.O. Box 1 Buffalo, NY 14240
1	Hughes Aircraft Company ATTN: T.E. Ward 8433 Fallbrook Avenue Canoga Park, CA 91303	1	Thiokol Corporation Elkton Division ATTN: W.N. Brundige P.O. Box 241 Elkton, MD 21921

DISTRIBUTION LIST

<u>No. Of Copies</u>	<u>Organization</u>	<u>No. Of Copies</u>	<u>Organization</u>
1	Thiokol Corporation Huntsville Division ATTN: R. Glick Huntsville, AL 35807	1	Brigham Young University Dept. of Chemical Engineering ATTN: M.W. Beckstead Provo, UT 84601
3	Thiokol Corporation Wasatch Division ATTN: S.J. Bennett P.O. Box 524 Brigham City, UT 84302	1	California Institute of Tech. Jet Propulsion Laboratory ATTN: MS 125/159 4800 Oak Grove Drive Pasadena, CA 91103
1	TRW ATTN: M.S. Chou MSR1-1016 1 Parke Redondo Beach, CA 90278	1	California Institute of Technology ATTN: F.E.C. Culick/ MC 301-46 204 Karman Lab. Pasadena, CA 91125
1	United Technologies ATTN: A.C. Eckbreth East Hartford, CT 06108	1	University of California, Berkeley Mechanical Engineering Dept. ATTN: J. Daily Berkeley, CA 94720
3	United Technologies Corp. Chemical Systems Division ATTN: R.S. Brown T.D. Myers (2 copies) P.O. Box 50015 San Jose, CA 95150-0015	1	University of California Los Alamos Scientific Lab. P.O. Box 1663, Mail Stop B216 Los Alamos, NM 87545
2	United Technologies Corp. ATTN: R.S. Brown R.O. McLaren P.O. Box 358 Sunnyvale, CA 94086	2	University of California, Santa Barbara Quantum Institute ATTN: K. Schofield M. Steinberg Santa Barbara, CA 93106
1	Universal Propulsion Company ATTN: H.J. McSpadden Black Canyon Stage 1 Box 1140 Phoenix, AZ 85029	2	University of Southern California Dept. of Chemistry ATTN: S. Benson C. Wittig Los Angeles, CA 90007
1	Veritay Technology, Inc. ATTN: E.B. Fisher 4845 Millersport Highway P.O. Box 305 East Amherst, NY 14051-0305	1	Case Western Reserve Univ. Div. of Aerospace Sciences ATTN: J. Tien Cleveland, OH 44135

DISTRIBUTION LIST

<u>No. Of Copies</u>	<u>Organization</u>	<u>No. Of Copies</u>	<u>Organization</u>
1	Cornell University Department of Chemistry ATTN: T.A. Cool Baker Laboratory Ithaca, NY 14853	3	Pennsylvania State University Applied Research Laboratory ATTN: K.K. Kuo H. Palmer M. Micci University Park, PA 16802
1	Univ. of Dayton Rsch Inst. ATTN: D. Campbell AFRPL/PAP Stop 24 Edwards AFB, CA 93523	1	Polytechnic Institute of NY Graduate Center ATTN: S. Lederman Route 110 Farmingdale, NY 11735
1	University of Florida Dept. of Chemistry ATTN: J. Winefordner Gainesville, FL 32611	2	Princeton University Forrestal Campus Library ATTN: K. Brezinsky I. Glassman P.O. Box 710 Princeton, NJ 08540
3	Georgia Institute of Technology School of Aerospace Engineering ATTN: E. Price W.C. Strahle B.T. Zinn Atlanta, GA 30332	1	Princeton University MAE Dept. ATTN: F.A. Williams Princeton, NJ 08544
1	University of Illinois Dept. of Mech. Eng. ATTN: H. Krier 144MEB, 1206 W. Green St. Urbana, IL 61801	1	Purdue University School of Aeronautics and Astronautics ATTN: J.R. Osborn Grissom Hall West Lafayette, IN 47906
1	Johns Hopkins University/APL Chemical Propulsion Information Agency ATTN: T.W. Christian Johns Hopkins Road Laurel, MD 20707	1	Purdue University Department of Chemistry ATTN: E. Grant West Lafayette, IN 47906
1	University of Michigan Gas Dynamics Lab Aerospace Engineering Bldg. ATTN: G.M. Faeth Ann Arbor, MI 48109-2140	2	Purdue University School of Mechanical Engineering ATTN: N.M. Laurendeau S.N.B. Murthy TSPC Chaffee Hall West Lafayette, IN 47906
1	University of Minnesota Dept. of Mechanical Engineering ATTN: E. Fletcher Minneapolis, MN 55455	1	Rensselaer Polytechnic Inst. Dept. of Chemical Engineering ATTN: A. Fontijn Troy, NY 12181

DISTRIBUTION LIST

<u>No. Of Copies</u>	<u>Organization</u>
1	Stanford University Dept. of Mechanical Engineering ATTN: R. Hanson Stanford, CA 94305
1	University of Texas Dept. of Chemistry ATTN: W. Gardiner Austin, TX 78712
1	University of Utah Dept. of Chemical Engineering ATTN: G. Flandro Salt Lake City, UT 84112
1	Virginia Polytechnic Institute and State University ATTN: J.A. Schetz Blacksburg, VA 24061

Aberdeen Proving Ground

Dir, USAMSAA
ATTN: AMXSU-D
AMXSU-MP, H. Cohen
Cdr, USATECOM
ATTN: AMSTE-TO-F
Cdr, CRDC, AMCCOM
ATTN: SMCCR-RSP-A
SMCCR-MU
SMCCR-SPS-IL

USER EVALUATION SHEET/CHANGE OF ADDRESS

This Laboratory undertakes a continuing effort to improve the quality of the reports it publishes. Your comments/answers to the items/questions below will aid us in our efforts.

1. BRL Report Number _____ Date of Report _____

2. Date Report Received _____

3. Does this report satisfy a need? (Comment on purpose, related project, or other area of interest for which the report will be used.) _____

4. How specifically, is the report being used? (Information source, design data, procedure, source of ideas, etc.) _____

5. Has the information in this report led to any quantitative savings as far as man-hours or dollars saved, operating costs avoided or efficiencies achieved, etc? If so, please elaborate. _____

6. General Comments. What do you think should be changed to improve future reports? (Indicate changes to organization, technical content, format, etc.) _____

CURRENT ADDRESS Name _____
 Organization _____
 Address _____
 City, State, Zip _____

7. If indicating a Change of Address or Address Correction, please provide the New or Correct Address in Block 6 above and the Old or Incorrect address below.

OLD ADDRESS Name _____
 Organization _____
 Address _____
 City, State, Zip _____

(Remove this sheet along the perforation, fold as indicated, staple or tape closed, and mail.)

----- FOLD HERE -----

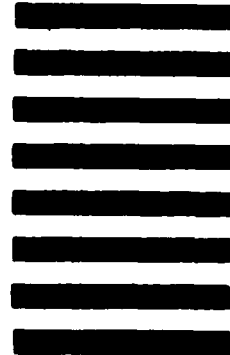
Director
U.S. Army Ballistic Research Laboratory
ATTN: SLCBR-DD-T
Aberdeen Proving Ground, MD 21005-5066



NO POSTAGE
NECESSARY
IF MAILED
IN THE
UNITED STATES

OFFICIAL BUSINESS
PENALTY FOR PRIVATE USE, \$300

BUSINESS REPLY MAIL
FIRST CLASS PERMIT NO 12062 WASHINGTON, DC
POSTAGE WILL BE PAID BY DEPARTMENT OF THE ARMY



Director
U.S. Army Ballistic Research Laboratory
ATTN: SLCBR-DD-T
Aberdeen Proving Ground, MD 21005-9989

----- FOLD HERE -----

END

DITIC

9 - 86